



Study of Thermal Generating Units of Multi-area Power System Connected to Grid and its Stability

Chandra Mohan Khan¹, Sukumar Chandra Konar², Chandan Kumar Chanda³

¹ Global Institute of Management & Technology, E. E. Dept. Krishnagar, Nadia-741102, W.B., India

^{2,3} Department of Electrical Engineering, Bengal Engineering & Science University, Shibpur, Howrah 711103.W.B., India.

Abstract— This paper presents an approach of the theory and practical applications involved in studding stability of a interconnected power system. It develops the necessary circuits and mathematical models as required in addition to describing the important role that modern computers can play in improving power-system performance. In an interconnected power system the change in real power affect mainly the system frequency, while variation of reactive power changes the voltage magnitude. Load frequency control loop controls the real power and it is important with the growth of interconnected systems and reactive power (or voltage magnitude) can be controlled by regulating excitation of alternator. In this paper, especially we are studying the load frequency control with variation of power of multi areas interconnected power system by using MATLAB SIMULINK technique.

Keywords- Thermal generating unit, computer programming, MATLAB SIMULINK, Stability study with controller and without controller.

I. INTRODUCTION

The frequency of a power system is dependent on real power balance. A change in real power demand at one point of a network is reflected throughout the system by a change in frequency. Therefore, system frequency provides a useful index to indicate system generation and load imbalance. Any short-term energy imbalance will result in an instantaneous change in system frequency as the disturbance is initially offset by the kinetic energy of the rotating plant. Significant loss in the generation without an adequate system response can produce extreme frequency excursions outside the working range of the plant. The control of frequency and power generation is commonly referred to as load–frequency control (LFC), which is a major function of automatic generation control (AGC) systems. For satisfactory operation of a power system, the frequency should be remained nearly constant [10].

II. FREQUENCY RESPONSE MODELING

Power systems have a highly non-linear and time-varying nature. However, for the purpose of frequency control synthesis and analysis in the presence of load disturbances, a simple low-order linearized model is used. In comparison with voltage and rotor angle dynamics, the dynamics affecting frequency response are relatively slow, in the range of seconds to minutes. To include both the fast and the slow power system dynamics [3], by considering generation and load dynamics in detail, complex numerical methods are needed to permit varying the simulation time step with the amount of fluctuation of system variables [4]. Neglecting the fast (voltage and angle) dynamics reduces the complexity of modeling, computation and data requirements. Analysis of the results is also simplified.

In this section, a simplified frequency response model for the described schematic block diagram in Fig.1 with one generator unit is described, and then the resulting model is generalized for an interconnected multi-machine power system in Sect.-III. The overall generator–load dynamic relationship between the incremental mismatch power ($\Delta P_m - \Delta P_L$) and the frequency deviation (Δf) can be expressed as,

$$\Delta P_m(t) - \Delta P_L(t) = 2H \frac{d\Delta f(t)}{dt} + D\Delta f(t) \quad \dots\dots(1)$$

Where, Δf and ΔP_m , are the frequency deviation, and the mechanical power changes respectively. The ΔP_L , H and D are the load change, inertia constant and load-damping coefficient respectively. The damping coefficient is usually expressed as a percent change in load for a 1% change in frequency. For example, a typical value of 1.5 for D means that a 1% change in frequency would cause a 1.5% change in load. Using the Laplace transform, equation- (1) can be written as, $\Delta P_m(s) - \Delta P_L(s) = 2H(s) \Delta f(s) + D\Delta f(s) \dots\dots\dots(2)$ Equation- (2) can be represented in a block diagram as in Fig.2.

This generator– load model can simply reduce the schematic block diagram of a closed-loop synchronous generator (Fig.1) as shown in Fig.3. Several low order models for representation of turbine and generator dynamics (G_t and G_g) have been proposed for use in power system frequency analysis and control design [5].

Slow system dynamics of the boiler and the fast generator dynamics are usually ignored in these models. Fig.4 represents the block diagram of the speed governor and the turbine of steam and hydraulic governors units appropriate for LFC synthesis/analysis. Here, R (and R_h) is the speed droop characteristic and shows the speed regulation due to governor action. T_g , T_t , T_r , T_{tr} , T_{gh} and T_{th} are generator–turbine time constants. Fig.5 shows a combination of the block diagrams of Figs.1,2 and 3a i.e., a block diagram representation for a non-reheat steam generator unit with associated frequency control loops (LFC system) comprising turbine, generator, governor, supplementary control and load.

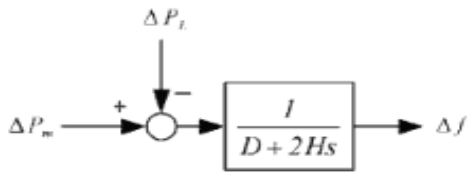


Fig.1: Block diagram of generator–load model.

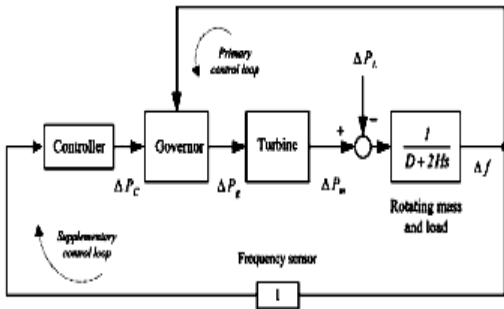


Fig.2: Reduced block diagram of Turbine and Generator

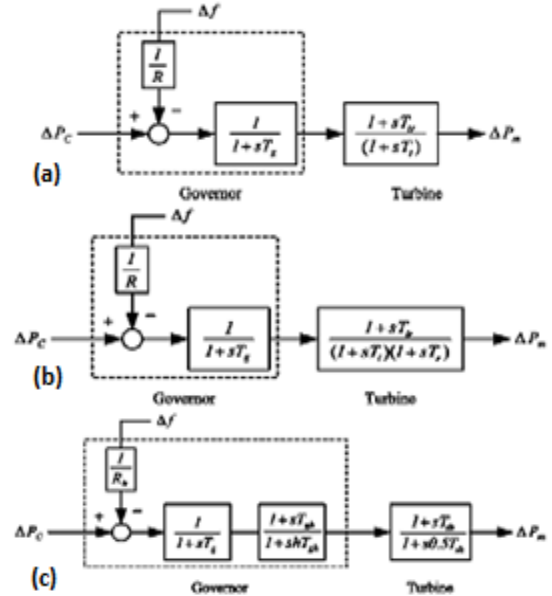


Fig.3: Block diagram of turbine-governor system; (a) non-reheat steam unit, (b) reheat steam unit and (c) hydraulic unit.

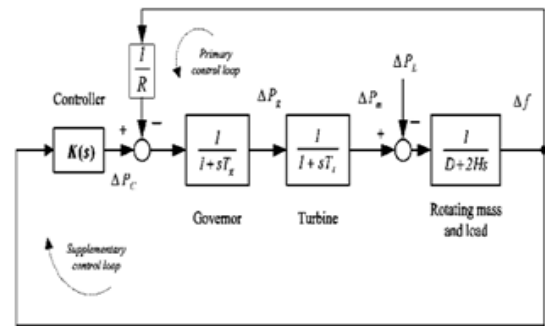


Fig.4: Block diagram model of governor with load frequency control loops for a non-reheat steam generator unit with supplementary control.

The dynamic response of the closed-loop system for a step load disturbance of 0.02 pu is plotted in Fig.6. For the sake of comparison, the frequency deviation of system without a supplementary control is plotted on the same figure. The systems parameters are given in Table - I for the MATLAB simulations work.

Table-I: Simulation data

Speed regulation	R=0.05
Frequency- sens. load coeff.	D=0.6
Inertia constant	H=5
Governor time constant	$T_g=0.2$ sec.
Turbine time constant	$T_t=0.5$ sec.
Controller gain	$K(s)=-7/s$

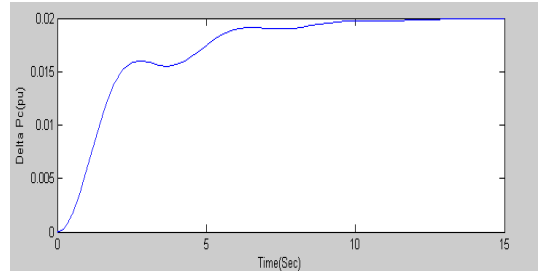


Fig.6: ΔP_c Vs. Time .

Fig.6: Dynamic response of the closed-loop system with (solid) and without (dotted) supplementary control

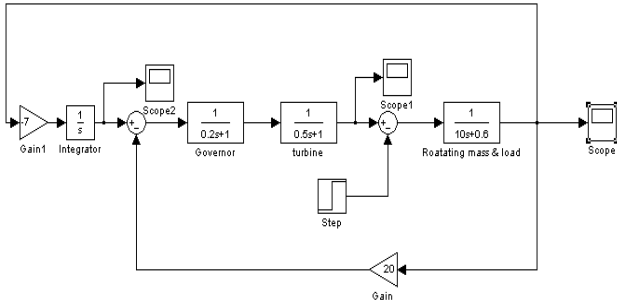


Fig. 5: simulation block diagram

III. FREQUENCY CONTROL IN AN INTERCONNECTED POWER SYSTEM

In order to conduct a frequency response analysis for an *isolated* power system in the presence of sudden load variation is usually the model of a multi-machine dynamic behavior by an equivalent single machine as shown in Fig.5. In this case, the proposed model can be used as an equivalent frequency response model for the whole multi-machine power system.

The equivalent model lumps the effects of system loads and generators into a single damping constant; the equivalent inertia constant is assumed to equal the sum of the inertia constant of all the generating units. Furthermore, it is assumed that the individual control loops and turbine-generators have the same regulation parameter and response characteristics. It should be reminded that the equivalent model is only useful to simplify the frequency response analysis of an isolated power system [7].

In an isolated power system, regulation of interchange power is not a control issue, and the LFC task is limited to restore the system frequency to the specified nominal value. In order to generalize the described model for interconnected power systems, the *control area* concept needs to be used, as it is a coherent area consisting of a group of generators and loads, where all the generators respond to changes in load or speed-changer settings, in unison. The frequency is assumed to be the same in all points of a control area.

A multi-area power system comprises areas that are interconnected by high voltage transmission lines or tie-lines. The trend of frequency measured in each control area is an indicator of the trend of the mismatch power in the

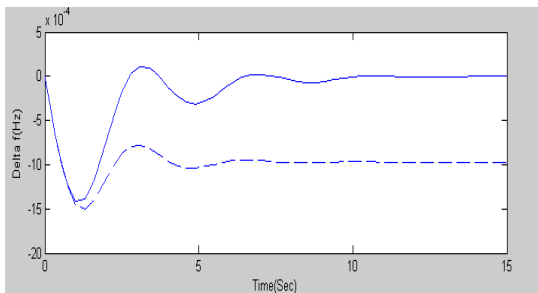


Fig.6 (a) Δf Vs. Time

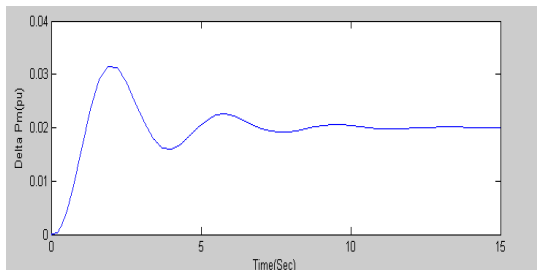


Fig.6(b) ΔP_m Vs. Time.

interconnection and not in the control area alone. The LFC system in each control area of an interconnected (multi-area) power system should control the interchange power with the other control areas as well as its local frequency. Therefore, the dynamic LFC system model (Fig.4) is to be modified by taking into account the tie-line power signal. For this purpose, consider Fig.7, which shows a power system with N -control areas.

The power flow on the tie-line from area 1 to area 2 is

$$P_{tie,12} = \frac{V_1 V_2}{X_{12}} \sin(\delta_1 - \delta_2) \dots\dots\dots(3)$$

where the tie-line reactance X_{12} , δ_1, δ_2 the power angles of equivalent machines and V_1, V_2 are the voltages at equivalent machine's of terminals of the area-1 and area-2.

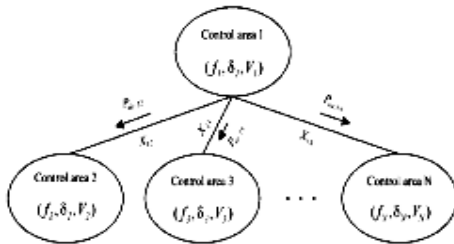


Fig.7: N-control areas power system

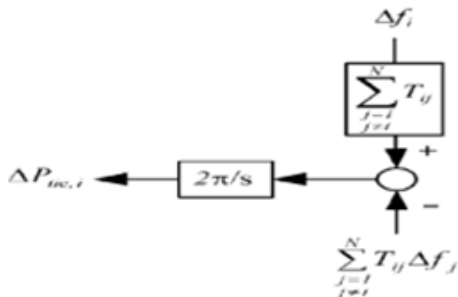


Fig.8: Tie-line power Change of control Area- i in N-control area power systems.

By linearizing (3) about an equilibrium point δ_1^0, δ_2^0

$$\Delta P_{tie,12} = T_{12} (\Delta \delta_1 - \Delta \delta_2), \dots\dots\dots(4)$$

Where, T_{12} is the synchronizing torque coefficient given by

$$T_{12} = \frac{|V_1| |V_2|}{X_{12}} \cos(\delta_1^0 - \delta_2^0). \dots\dots\dots(5)$$

Considering the relationship between area power angle and frequency, (4) can be written as

$$\Delta P_{tie,12} = 2\pi T_{12} (\int \Delta f_1 - \int \Delta f_2), \dots\dots\dots(6)$$

Where, Δf_1 and Δf_2 are frequency deviations in areas-1 and area-2 respectively. The Laplace transform of (6) is $\Delta P_{tie,12}(s)$ which is obtained as,

$$\Delta P_{tie,12}(s) = \frac{2\pi}{s} T_{12} (\Delta f_1(s) - \Delta f_2(s)). \dots\dots\dots(7)$$

Similarly, the tie-line power changes between areas-1 and area-3 is given as,

$$\Delta P_{tie,13}(s) = \frac{2\pi}{s} T_{13} (\Delta f_1(s) - \Delta f_3(s)). \dots\dots\dots(8)$$

Considering (7) and (8), the total tie-line power change between area-1 and the other two areas (2) and (3) can be calculated as

$$\Delta P_{tie,1} = \Delta P_{tie,12} + \Delta P_{tie,13} = \frac{2\pi}{s} \left[\sum_{j=2,3} T_{1j} \Delta f_1 - \sum_{j=2,3} T_{1j} \Delta f_j \right] \dots\dots\dots(9)$$

Similarly, for N control areas (Fig.7), the total tie-line power change between area-1 and other areas is

$$\Delta P_{tie,i} = \sum_{j=1, j \neq i}^N \Delta P_{tie,ij} = \frac{2\pi}{s} \left[\sum_{j=1, j \neq i}^N T_{ij} \Delta f_i - \sum_{j=1, j \neq i}^N T_{ij} \Delta f_j \right] \dots\dots\dots(10)$$

Equation (10) is represented in the form of a block diagram in Fig.8. The effect of changing the tie-line power for an area is equivalent to changing the load of that area. Therefore, the $\Delta P_{tie,i}$ must be added to the mechanical power change ($\Delta P_{m,i}$) and area load change (ΔP_L) using an appropriate sign. A combination of block diagrams (Figs.4 and Fig.-7) create a simplified block diagram for control area i in an N -control area power system (Fig.8).

The next point to consider is the supplementary control loop in the presence of a tie-line. In the case of an isolated control area, this loop is performed by a feedback from a control area frequency deviation through a simple dynamic controller (Fig.4). As in Fig.5, this structure provides a sufficient supplementary control action to force the steady-state frequency deviation to zero.

In a multi-area power system, in addition to regulating area frequency, the supplementary control should maintain the net interchange of power of the neighboring areas at scheduled values [17]. This is generally accomplished by adding a tie-line flow deviation to the frequency deviation in the supplementary feedback loop. A suitable linear combination of frequency and tie-line power changes for area-1, is known as the *area control error* (ACE)

$$ACE_i = \Delta P_{tie,i} + \beta_i \Delta f_i, \dots\dots\dots(11)$$

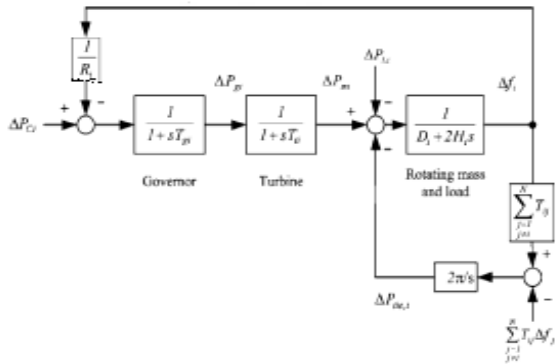


Fig.9: Block diagram of control Area - i

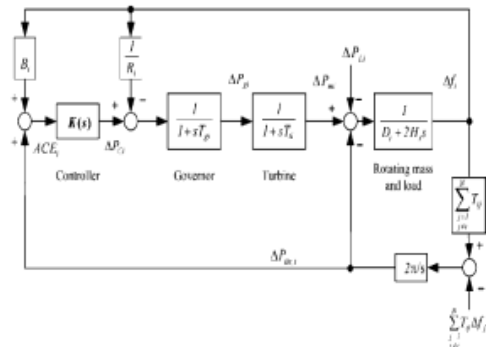


Fig.10: Control Area - i with suppl. Control

$$\beta_i = \frac{1}{R_i} + D_i \quad \dots\dots\dots (12)$$

Where β_i is a bias factor and its suitable value can be computed as follows [1]. The block diagram is shown in Fig.10, which illustrates how supplementary control is implemented by using (11).

The effects of local load changes and interface with other areas are properly considered as two input signals. Each control area monitors its own tie-line power flow and frequency at the area control centre. The ACE signal is computed and allocated to the controller $K(s)$. Finally, the resulting control action signal is applied to the turbine-governor unit. Therefore, it is expected that the supplementary control shown in Fig.9 can ideally meet the basic LFC objectives and maintain area frequency and tie-line interchange at scheduled values.

To illustrate LFC system behavior in a multi-area power system, consider two identical interconnected control areas as shown in Fig.11. The simulation parameters are given in Table-II. Fig.12 shows the simulation block diagram of two areas control without controller. The system dynamic

response following a simultaneous 0.01-pu to 0.05-pu load step disturbance in control areas-1 are shown in Figs. 13(a),(b),(c) and Figs.15(a),(b),(c) respectively.

This figure shows that the power to compensate the tie-line power change initially comes from all areas to respond to the step load increase in areas-1 and area- 2, and results in a frequency drop, sensed by the speed governors of all generators. However, after a few seconds (at steady state), the additional powers against the local load changes come only from areas-1 and area- 2.

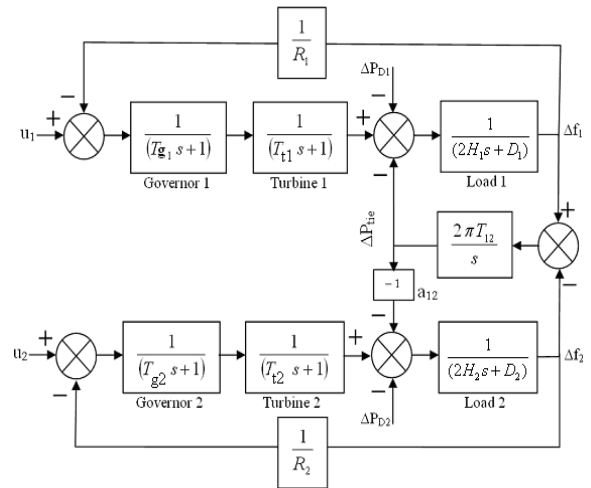


Fig.11: Two interconnected power systems.

A two-area system connected by a tie line has the following parameters on a 1000 MVA common base.

Table-II: LFC simulation parameters

Parameter	Area-1	Area-2
Speed regulation	$R_1 = 0.05$ Hz/pu	$R_2 = 0.0625$ Hz/pu
Frequency-sens. Load coeff.	$D_1 = 0.6$ pu/Hz	$D_2 = 0.9$ pu/Hz
Inertia constant	$H_1 = 5$	$H_2 = 4$
Base power	1000 MVA	1000 MVA
Governor time constant	$T_{g1} = 0.2$ sec	$T_{g2} = 0.3$ sec
Turbine time constant	$T_{t1} = 0.5$ sec	$T_{t2} = 0.6$ sec
Synchronizing torque coefficient	$T_{12} = 0.699$ sec	$T_{21} = 0.699$ sec

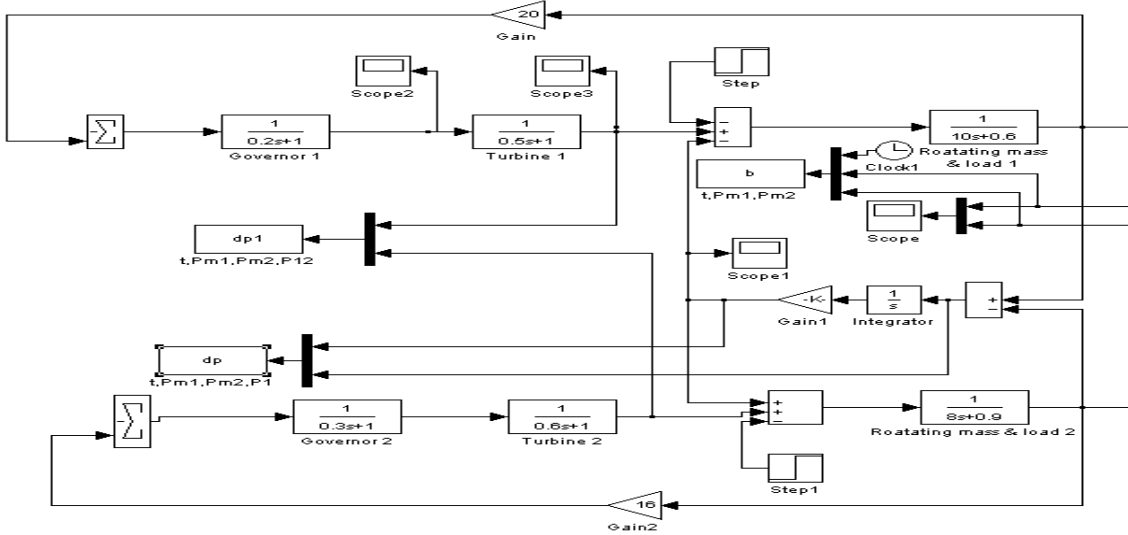


Fig.12: Simulation Block diagram of two area control without controller

IV. SIMULATION RESULT.

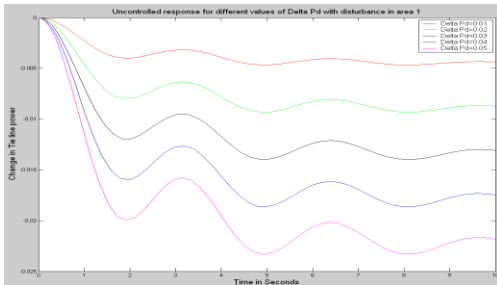
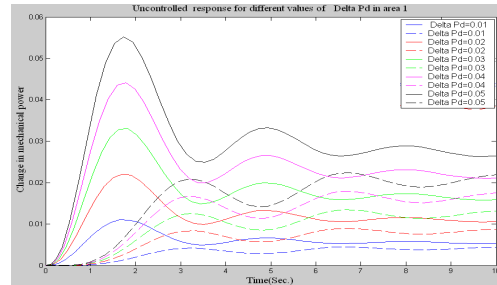


Fig. 13(a) : Variation of tie line power deviations Vs. Time.



Fi.13(c) : Variation of mech. Power Vs. Time, in Area -1 & area-2(dotted)

Fig. 13(a),(b),(c) : Simulation results of dynamic response following simultaneous 0.01-pu to 0.05 pu load step disturbance in area-1 (solid-line) and area-2 (dotted-line) without controller.

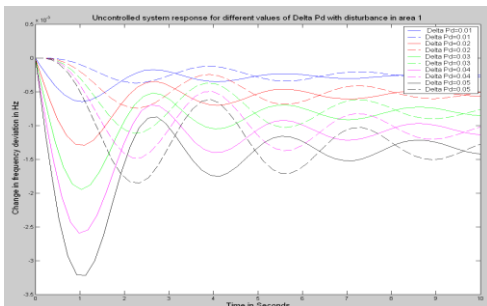


Fig. 13(b): Variation of freq. Vs. Time, in area-1(solid), And in area-2 (dotted)

Table-III of Annexure shows the uncontrolled system for change of frequency $\Delta f_1, \Delta f_2$, deviation, change of mechanical power $\Delta P_{m1}, \Delta P_{m2}$, change of dP_{tie}/dt tie line power ΔP_{tie} and change of rate of tie line power, of area-land area-2 respectively with disturbance $\Delta pd=0.03$ in area-1 ($t=10$ sec). Table- IV of annexure shows the uncontrolled system for change of frequencies $\Delta f_1, \Delta f_2$, and change of mechanical power $\Delta P_{m1}, \Delta P_{m2}$, and rate of change of tie line power dP_{tie}/dt of area-1, area-2 respectively.

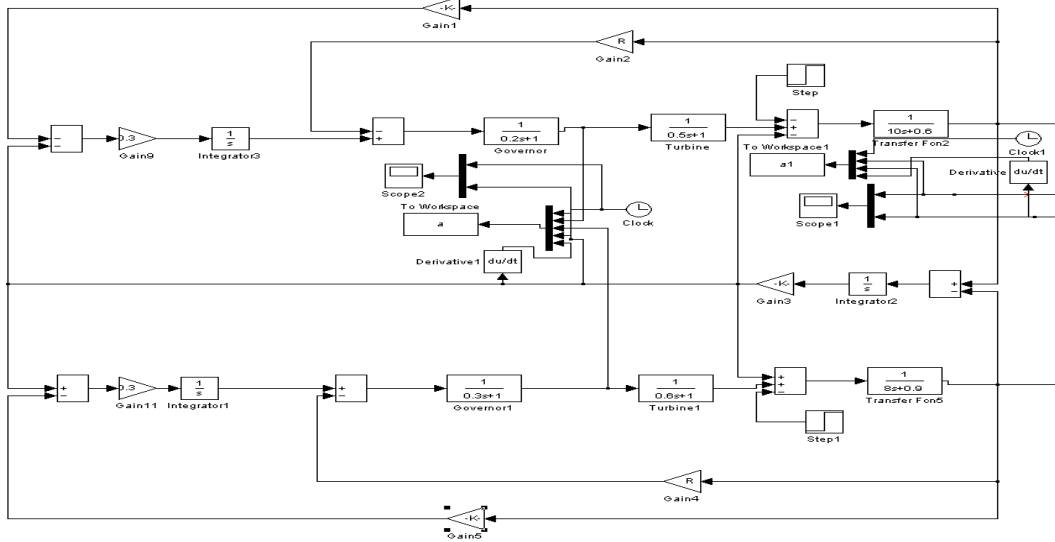


Fig.14: Simulation block diagram of two-areas control with Integral Controller follows Simulation Results.

A two-area system connected by a tie line has the following parameters in Table- V and simulation results Fig.15 on a 1000 MVA common base.

Table - V

Parameter	Area-1	Area-2
Speed regulation	$R_1 = 0.05$ Hz/pu	$R_2 = 0.0625$ Hz/pu
Frequency-sens. Load coeff.	$D_1 = 0.6$ pu/Hz	$D_2 = 0.9$ pu/Hz
Inertia constant	$H_1 = 5$	$H_2 = 4$
Base power	1000 MVA	1000 MVA
Governor time constant	$T_{g1} = 0.2$ sec	$T_{g2} = 0.3$ sec
Turbine time constant	$T_{t1} = 0.5$ sec	$T_{t2} = 0.6$ sec
Synchronizing torque coefficient	$T_{12} = 0.699$ sec	$T_{21} = 0.699$ sec

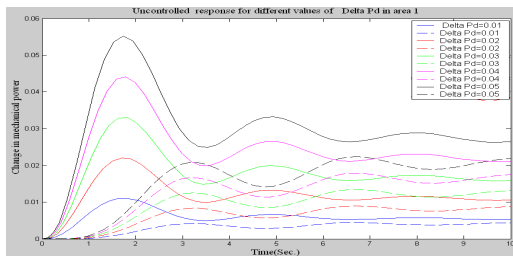


Fig. 15(a): ΔP_{tie} (Variation of tie line Power) Vs. Time.

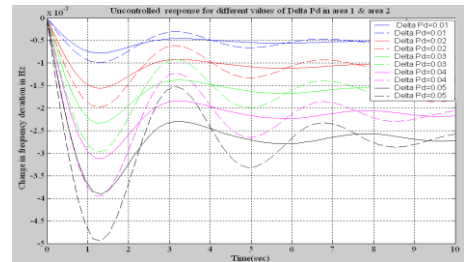


Fig. 15(b): Δf (Variation of frequency) in area-1 (solid) and area-2 (dotted) Vs. Time.

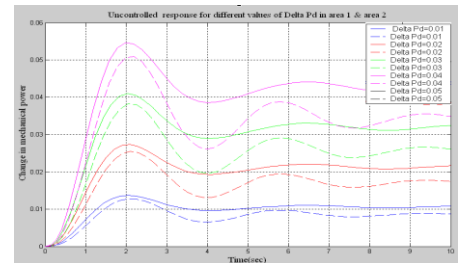


Fig.15(c): ΔP_m (Variation mech. Power) in area-1 (solid) & area-2 (dotted) Vs. Time

Fig. 15: Simulation results of dynamic response following simultaneous 0.01-pu to 0.05 pu load step disturbance in area-1 (solid-line) and area-2 (dotted-line) with Integral Controller.

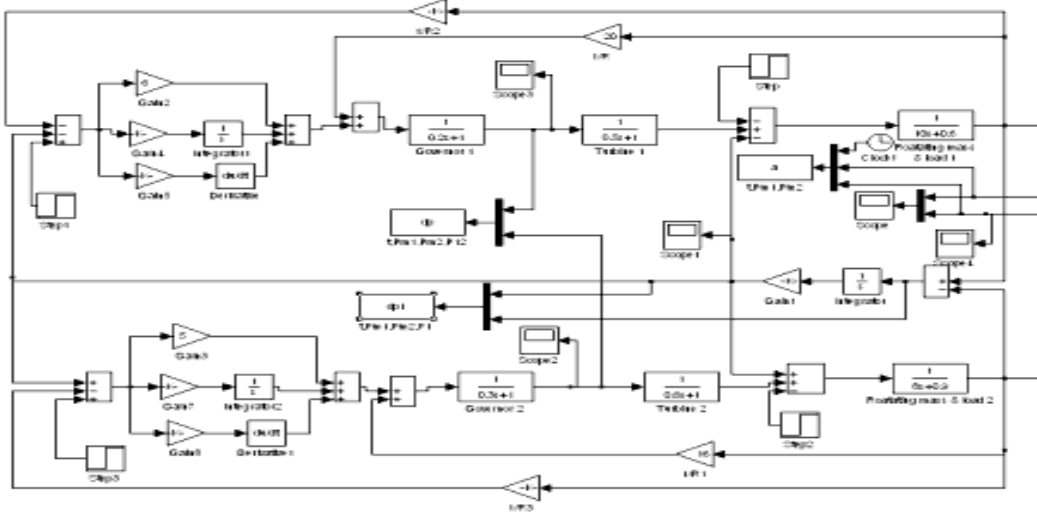


Fig. 16: Simulation block diagram of two area control with PID Controller

V. SIMULATION RESULTS.

Fig.16 shows the Simulation block diagram of two area control with PID Controller. The power compensate the tie line power change initially fed from all areas to respond to the step load increases in area-1 and area-2, and results in a frequency drop sensed by the speed governors of all generators. However, after a few seconds (at steady state), the additional power against local load changes come only from area- 1 and area-2. The simulation results are as follows,

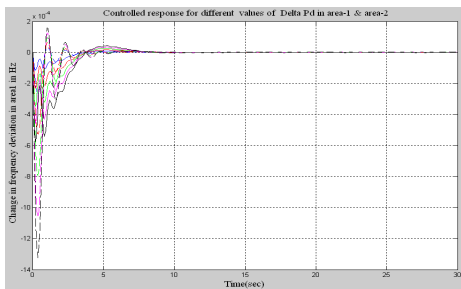
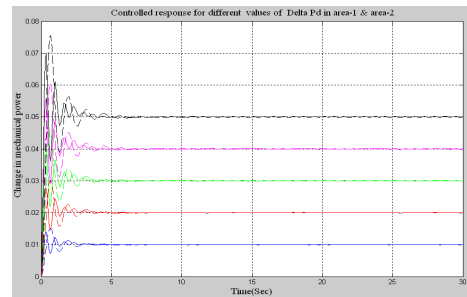
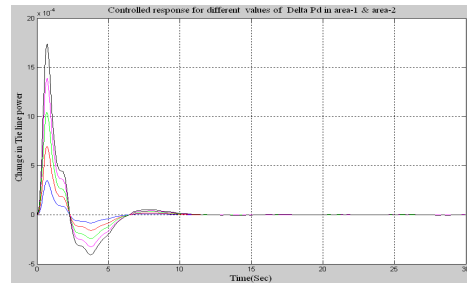


Fig. 17(a): Plot: Δf (changes of frequency) Vs. Time .



17(b) Plot: ΔP_m (changes of mechanical power) Vs. Time .



17(c) Plot: ΔP_{tie} (Changes in Tie line power) Vs. Time .

Fig. 17: Time response of controlled systems for different values of ΔP_d in area-1

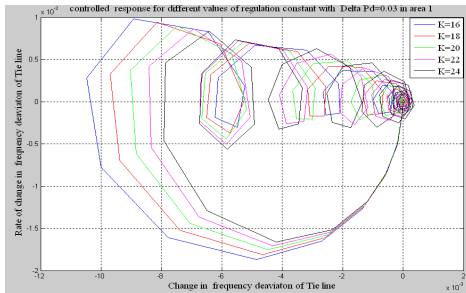


Fig.18: Phase-Plane trajectories of controlled system for different values of regulation constants with disturbance $\Delta P_d=0.03$ in area-1. Plot: ΔP_{tie} Vs. dP_{tie}/dt .

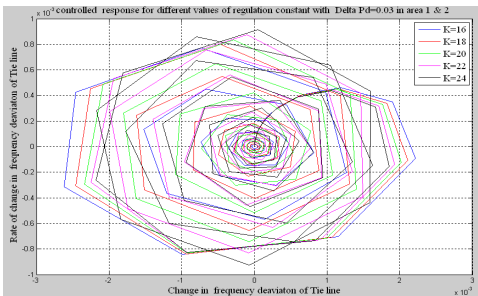


Fig.19: Phase-Plane trajectories of controlled system for different values of regulation constants with disturbance $\Delta p_d=0.03$ in area-1 and area-2. Plot: ΔP_{tie} Vs. dP_{tie}/dt .

The Phase-plane trajectory-curve changes when we compare for area-1 and both area-1, area-2. Table-V of controlled two area system (parameters are same) for change of frequencies $\Delta f_1, \Delta f_2$, change of mechanical power $\Delta P_{m1}, \Delta P_{m2}$, change of tie line power ΔP_{tie} and rate of tie line power dP_{tie}/dt of area -1 and area- 2 respectively with disturbance $\Delta p_d = 0.03$ in both area -1 and area-2.

VI. CONCLUSION.

Two area interconnected power system is represented using new state variables namely frequency deviation and its derivative as state variables in both the areas without integral control of frequency in each case. The static errors of the frequency deviations and tie line power deviations are increasing with increase in load changes without controller.

When the controller is placed in area-1 for change of loads in that area the maximum negative overshoot Δf_1 is more compared to that of Δf_2 for a particular load change. Whereas the tie line power deviations are also oscillatory and reaching zero steady state value.

It is observed that when parameters of two area are same and with same value of disturbances, then the tie line power does not vary.

The case study with controllers in both the areas for a load change in area- 1 indicates that the responses are oscillatory. However the magnitudes of the overshoots are less compared to that of the other case. It is also observed that the values of the maximum overshoots are increasing with increase in load changes. The settling times for frequency deviations and tie line power deviations are less with this scheme. Considering the transient behavior of the interconnected power system the scheme with two PID controllers is a better option than integral controller.

REFERENCES

- [1] J.VAN AMERONGEN, H.W.M BAREND, P.J.BUYS AND G.HODERD “ Modeling and control of 180 MW Power system” .IEEE Transaction on Automatic control, vol, AC-31 No.9 September 1986.
- [2] O. P. Malik, G. S. Hope, Y. M. Gorski, V. A. Uskakov, and A. L. Rackevich, Experimental studies on adaptive microprocessor stabilizers for synchronous generators, in *IFAC Power Syst. Power Plant Control*, Beijing, China, 125–130, 1986.
- [3] Y. Guo, D. J. Hill, and Y. Wang, Global transient stability and voltage regulation for power systems, *IEEE Trans. Power Syst.*, 16(4), 678–688, 2001.
- [4] K. T. Law, D. J. Hill, and N. R. Godfrey, “Robust co-ordinated AVR-PSS design,” *IEEE Trans on Power Systems*, 9(3), 1218–1225, 1994.
- [5] I. Kamwa, R. Grondin, and Y. Hebert, Wide-area measurement based stabilizing control of large power systems: A decentralized hierarchical approach, *IEEE Trans. Power Syst.*, 16(1), 136–153, 2001.
- [6] J. A. Momoh, *Electric Power Distribution, Automation, Protection and Control*. New York, NY: CRC, 2008.26. B. Pal and B. Chaudhuri, *Robust Control in Power Systems*. New York, NY: Springer, 2005.
- [7] H. Bevrani and T. Hiyama, Power system dynamic stability and voltage regulation enhancement using an optimal gain vector, *Control Eng. Pract.*, 16(9), 1109–1119, 2008.
- [8] J. A. Pecas Lopes, N. Hatziaegyriou, J. Mutale, et al., Integrating distributed generation into electric power systems: A review of drivers, challenges and opportunities, *Electr. Power Syst. Res.*, 77, 1189–1203, 2007.



International Journal of Recent Development in Engineering and Technology

Website: www.ijrdet.com (ISSN 2347-6435(Online) Volume 2, Issue 2, February 2014)

- [9] CIGRE Task Force 38.01.07 on Power System Oscillations, *Analysis and Control of Power System Oscillations*, CIGRE Technical Brochure, no. 111, Dec. 1996.
- [10] P. Kundur, D. C. Lee, J. P. Bayne, and P. L. Dandeno, Impact of turbine generator controls on unit performance under system disturbance conditions, *IEEE Trans. Power App. Syst.*, 104(6), 1262–1267, 1985; Bowman, M., Debray, S. K., and Peterson, L. L. 1993. Reasoning about naming systems. .
- [11] R. R. Shoultz and J. A. J. Ibarra, Multi-area adaptive LFC developed for a comprehensive AGC simulator, *IEEE Trans. Power App. Syst.*, vol. 8, no. 2, pp. 541–547, 1993
- [12] N. Jaleeli, L. S. Vanslyck, NERC's new control performance standards, *IEEE Trans. Power Syst.*, vol. 14, no. 3, pp. 1092–1099, 1999.
- [13] M. Yao, R. R. Shoultz, R. Kelm, AGC logic based on NERC's new control performance standard and disturbance control standard, *IEEE Trans. Power Syst.*, vol. 15, no. 2, pp. 852–857, 2000.
- [14] N. Hoonchareon, C. M. Ong, R. A. Kramer, Feasibility of decomposing ACE1 to identify the impact of selected loads on CPS1 and CPS2, *IEEE Trans. Power Syst.*, vol. 17, no. 3, pp. 752–756, 2002.
- [15] L. R. C. Chien, N. Hoonchareon, C. M. Ong, R. A. Kramer, Estimation of β for adaptive frequency bias setting in load frequency control, *IEEE Trans. Power Syst.*, vol. 18, no. 2, pp. 904–911, 2003.
- [16] B. Stojkovic, An original approach for load–frequency control – the winning solution in the second UCTE synchronous zone, *Electr. Power Syst. Res.*, vol. 69, pp. 59–68, 2004.
- [17] H. Bevrani, T. Hiyama, Y. Mitani, K. Tsuji, Automatic generation control: A decentralized robust approach, *Intell. Autom. Soft Comput. J.*, vol. 13, no. 3, pp. 273–287, 2007.
- [18] A. Rubaai and V. Udo, An adaptive control scheme for LFC of multiarea power systems. Part I: Identification and functional design, Part-II: Implementation and test results by simulation, *Electr. Power Syst. Res.*, vol. 24, no. 3, pp. 183–197, 1992.
- [19] Y. Hain, R. Kulesky, G. Nudelman, Identification-based power unit model for load– frequency control purposes, *IEEE Trans. Power Syst.*, vol. 15, no. 4, pp. 1313–1321, 2000.
- [20] M. Aldeen and H. Trinh, Load frequency control of interconnected power systems via constrained feedback control schemes, *Int. J. Comput. Electr. Eng.*, vol. 20, no. 1, pp. 71–88, 1994.
- [21] D. Das, M. L. Kothari, D. P. Kothari, J. Nanda, Variable structure control strategy to automatic generation control of interconnected reheat thermal systems, *Proc. Inst. Electr. Eng. Control Theory Appl.*, vol. 138, no. 6, pp. 579–585, 1991.
- [22] D. Rerkpreedapong, A. Hasanovic, A. Feliachi, Robust load frequency control using genetic algorithms and linear matrix inequalities, *IEEE Trans. Power Syst.*, vol. 18, no. 2, pp. 855–861, 2003.
- [23] H. Bevrani, T. Hiyama, Y. Mitani, K. Tsuji, Automatic generation control: A decentralized robust approach, *Intell. Autom. Soft Comput. J.*, vol. 13, no. 3, pp. 273–287, 2007.
- [24] Y. Hain, R. Kulesky, G. Nudelman, Identification-based power unit model for load– frequency control purposes, *IEEE Trans. Power Syst.*, vol. 15, no. 4, pp. 1313–1321, 2000.
- [25] D. Rerkpreedapong, A. Hasanovic, A. Feliachi, Robust load frequency control using genetic algorithms and linear matrix inequalities, *IEEE Trans. Power Syst.*, vol. 18, no. 2, pp. 855–861, 2003.
- [26] Y. L. Karnavas and D. P. Papadopoulos, AGC for autonomous power system using combined intelligent techniques, *Electr. Power Syst. Res.*, vol. 62, pp. 225–239, 2002.
- [27] A. Demiroren and E. Yesil, Automatic generation control with fuzzy logic controllers in the power system including SMES units, *Electr. Power Energy Syst.*, vol. 26, pp. 291–305, 2004
- [28] E. Yesil, M. Guzelkaya, I. Eksin, Self tuning fuzzy PID type load frequency controller, *Energy Convers. Manage.*, vol. 45, pp. 377–390, 2004.
- [29] C. S. Chang, W. Fu, F. Wen, Load frequency controller using genetic algorithm based fuzzy gain scheduling of PI controller, *Electr. Mach. Power Syst.*, vol. 26, pp. 39–52, 1998.

ANNEXURE

Table – III

t	Δf_1	Δf_2	ΔP_{m1}	ΔP_{m2}	ΔP_{tie}	$\Delta P_{tie}/\Delta t$
0.0000	-0.0000	-0.0000	0.0000	0.0000	0.0000	0.0000
0.0067	-0.0000	-0.0000	0.0000	0.0000	0.0000	0.0000
0.0402	-0.0001	-0.0002	0.0000	0.0000	0.0000	0.0000
0.1671	-0.0005	-0.0006	0.0004	0.0002	0.0000	0.0001
0.2938	-0.0009	-0.0011	0.0016	0.0010	0.0001	0.0002
0.4400	-0.0013	-0.0016	0.0042	0.0028	0.0003	0.0003
0.6331	-0.0017	-0.0021	0.0093	0.0066	0.0006	0.0004
0.8331	-0.0020	-0.0026	0.0159	0.0119	0.0010	0.0005
1.0331	-0.0023	-0.0029	0.0228	0.0179	0.0015	0.0006
1.2331	-0.0023	-0.0030	0.0292	0.0240	0.0021	0.0006
1.4331	-0.0023	-0.0029	0.0344	0.0294	0.0026	0.0006
1.6331	-0.0022	-0.0028	0.0381	0.0338	0.0031	0.0005
1.8331	-0.0021	-0.0025	0.0403	0.0368	0.0035	0.0004
2.0331	-0.0019	-0.0021	0.0410	0.0382	0.0038	0.0002
2.2331	-0.0018	-0.0018	0.0405	0.0381	0.0039	0.0000
2.4331	-0.0016	-0.0015	0.0392	0.0367	0.0039	-0.0001
2.6331	-0.0015	-0.0012	0.0374	0.0343	0.0037	-0.0003
2.8331	-0.0014	-0.0010	0.0353	0.0314	0.0034	-0.0004
3.0331	-0.0014	-0.0009	0.0334	0.0282	0.0030	-0.0005
3.2331	-0.0014	-0.0009	0.0318	0.0252	0.0026	-0.0005
3.4331	-0.0014	-0.0010	0.0305	0.0227	0.0022	-0.0004
3.6331	-0.0014	-0.0011	0.0296	0.0208	0.0019	-0.0003
3.8331	-0.0014	-0.0013	0.0291	0.0198	0.0017	-0.0001
4.0331	-0.0015	-0.0015	0.0289	0.0196	0.0017	0.0000
4.2331	-0.0015	-0.0017	0.0291	0.0201	0.0017	0.0001
4.4331	-0.0015	-0.0018	0.0294	0.0212	0.0019	0.0003
4.6331	-0.0016	-0.0019	0.0298	0.0227	0.0022	0.0003
4.8331	-0.0016	-0.0020	0.0303	0.0244	0.0025	0.0004
5.0331	-0.0016	-0.0020	0.0308	0.0260	0.0028	0.0004
5.2331	-0.0016	-0.0020	0.0313	0.0274	0.0031	0.0003
5.4331	-0.0017	-0.0019	0.0318	0.0284	0.0033	0.0002
5.6331	-0.0017	-0.0018	0.0322	0.0290	0.0035	0.0001
5.8331	-0.0017	-0.0017	0.0326	0.0291	0.0035	0.0000
6.0331	-0.0017	-0.0016	0.0328	0.0289	0.0035	-0.0001
6.2331	-0.0017	-0.0015	0.0330	0.0282	0.0034	-0.0002
6.4331	-0.0016	-0.0014	0.0331	0.0274	0.0032	-0.0002
6.6331	-0.0016	-0.0014	0.0330	0.0265	0.0030	-0.0002
6.8331	-0.0016	-0.0014	0.0329	0.0256	0.0028	-0.0002
7.0331	-0.0016	-0.0014	0.0327	0.0248	0.0027	-0.0002
7.2331	-0.0016	-0.0015	0.0324	0.0242	0.0025	-0.0001
7.4331	-0.0016	-0.0015	0.0321	0.0239	0.0025	-0.0000
7.6331	-0.0015	-0.0016	0.0318	0.0238	0.0025	0.0000
7.8331	-0.0015	-0.0016	0.0316	0.0240	0.0025	0.0001
8.0331	-0.0015	-0.0017	0.0313	0.0243	0.0026	0.0001
8.2331	-0.0016	-0.0017	0.0312	0.0247	0.0027	0.0001
8.4331	-0.0016	-0.0017	0.0311	0.0253	0.0028	0.0001
8.6331	-0.0016	-0.0017	0.0312	0.0257	0.0030	0.0001
8.8331	-0.0016	-0.0017	0.0313	0.0262	0.0031	0.0001
9.0331	-0.0016	-0.0017	0.0315	0.0265	0.0031	0.0001
9.2331	-0.0016	-0.0016	0.0317	0.0266	0.0032	0.0000

Table – IV

t	Δf_1	Δf_2	ΔP_{m1}	ΔP_{m2}	ΔP_{tie}	$\Delta P_{tie}/\Delta t$
0.0000	-0.0000	-0.0000	0.0000	0.0000	0.0000	0.0000
0.0067	-0.0000	-0.0000	0.0000	0.0000	0.0000	0.0000
0.0402	-0.0001	-0.0002	0.0000	0.0000	0.0000	0.0000
0.1671	-0.0005	-0.0006	0.0004	0.0002	0.0000	0.0001
0.2938	-0.0009	-0.0011	0.0016	0.0010	0.0001	0.0002
0.4400	-0.0013	-0.0016	0.0042	0.0028	0.0003	0.0003
0.6331	-0.0017	-0.0021	0.0093	0.0066	0.0006	0.0004
0.8331	-0.0020	-0.0026	0.0159	0.0119	0.0010	0.0005
1.0331	-0.0023	-0.0029	0.0228	0.0179	0.0015	0.0006
1.2331	-0.0023	-0.0030	0.0292	0.0240	0.0021	0.0006
1.4331	-0.0023	-0.0029	0.0344	0.0294	0.0026	0.0006
1.6331	-0.0022	-0.0028	0.0381	0.0338	0.0031	0.0005
1.8331	-0.0021	-0.0025	0.0403	0.0368	0.0035	0.0004
2.0331	-0.0019	-0.0021	0.0410	0.0382	0.0038	0.0002
2.2331	-0.0018	-0.0018	0.0405	0.0381	0.0039	0.0000
2.4331	-0.0016	-0.0015	0.0392	0.0367	0.0039	-0.0001
2.6331	-0.0015	-0.0012	0.0374	0.0343	0.0037	-0.0003
2.8331	-0.0014	-0.0010	0.0353	0.0314	0.0034	-0.0004
3.0331	-0.0014	-0.0009	0.0334	0.0282	0.0030	-0.0005
3.2331	-0.0014	-0.0009	0.0318	0.0252	0.0026	-0.0005
3.4331	-0.0014	-0.0010	0.0305	0.0227	0.0022	-0.0004
3.6331	-0.0014	-0.0011	0.0296	0.0208	0.0019	-0.0003
3.8331	-0.0014	-0.0013	0.0291	0.0198	0.0017	-0.0001
4.0331	-0.0015	-0.0015	0.0289	0.0196	0.0017	0.0000
4.2331	-0.0015	-0.0017	0.0291	0.0201	0.0017	0.0001
4.4331	-0.0015	-0.0018	0.0294	0.0212	0.0019	0.0003
4.6331	-0.0016	-0.0019	0.0298	0.0227	0.0022	0.0003
4.8331	-0.0016	-0.0020	0.0303	0.0244	0.0025	0.0004
5.0331	-0.0016	-0.0020	0.0308	0.0260	0.0028	0.0004
5.2331	-0.0016	-0.0020	0.0313	0.0274	0.0031	0.0003
5.4331	-0.0017	-0.0019	0.0318	0.0284	0.0033	0.0002
5.6331	-0.0017	-0.0018	0.0322	0.0290	0.0035	0.0001
5.8331	-0.0017	-0.0017	0.0326	0.0291	0.0035	0.0000
6.0331	-0.0017	-0.0016	0.0328	0.0289	0.0035	-0.0001
6.2331	-0.0017	-0.0015	0.0330	0.0282	0.0034	-0.0002
6.4331	-0.0016	-0.0014	0.0331	0.0274	0.0032	-0.0002
6.6331	-0.0016	-0.0014	0.0330	0.0265	0.0030	-0.0002
6.8331	-0.0016	-0.0014	0.0329	0.0256	0.0028	-0.0002
7.0331	-0.0016	-0.0014	0.0327	0.0248	0.0027	-0.0002
7.2331	-0.0016	-0.0015	0.0324	0.0242	0.0025	-0.0001
7.4331	-0.0016	-0.0015	0.0321	0.0239	0.0025	-0.0000
7.6331	-0.0015	-0.0016	0.0318	0.0238	0.0025	0.0000
7.8331	-0.0015	-0.0016	0.0316	0.0240	0.0025	0.0001
8.0331	-0.0015	-0.0017	0.0313	0.0243	0.0026	0.0001
8.2331	-0.0016	-0.0017	0.0312	0.0247	0.0027	0.0001
8.4331	-0.0016	-0.0017	0.0311	0.0253	0.0028	0.0001
8.6331	-0.0016	-0.0017	0.0312	0.0257	0.0030	0.0001
8.8331	-0.0016	-0.0017	0.0313	0.0262	0.0031	0.0001
9.0331	-0.0016	-0.0017	0.0315	0.0265	0.0031	0.0001
9.2331	-0.0016	-0.0016	0.0317	0.0266	0.0032	0.0000